

An asymptotic-giant-branch star in the progenitor system of a type Ia supernova

Mario Hamuy¹, M. M. Phillips², Nicholas B. Suntzeff³, José Maza⁴, L. E. González⁴, Miguel Roth², Kevin Krisciunas², Nidia Morrell², E. M. Green⁵, S. E. Persson¹ & P. J. McCarthy¹

¹Carnegie Observatories, 813 Santa Barbara Street, Pasadena, California 91101, USA

²Las Campanas Observatory, Carnegie Observatories, Casilla 601, and

³Cerro Tololo Inter-American Observatory, National Optical Astronomy Observatories, Casilla 603, La Serena, Chile

⁴Departamento de Astronomía, Universidad de Chile, Casilla 36-D, Santiago, Chile

⁵University of Arizona, Steward Observatory, Tucson, Arizona 85721, USA

Stars that explode as supernovae come in two main classes. A type Ia supernova is recognized by the absence of hydrogen and the presence of elements such as silicon and sulphur in its spectrum; this class of supernova is thought to produce the majority of iron-peak elements in the Universe. They are also used as precise 'standard candles' to measure the distances to galaxies. While there is general agreement that a type Ia supernova is produced by an exploding white dwarf star¹, no progenitor system has ever been directly observed. Significant effort has gone into searching for circumstellar material to help discriminate between the possible kinds of progenitor systems², but no such material has hitherto been found associated with a type Ia supernova³. Here we report the presence of strong hydrogen emission associated with the type Ia supernova SN2002ic, indicating the presence of large amounts of circumstellar material. We infer from this that the progenitor system contained a massive asymptotic-giant-branch star that lost several solar masses of hydrogen-rich gas before the supernova explosion.

SN2002ic was discovered before or near maximum light by the Nearby Supernova Factory search⁴. It appeared ~4 arcsec west of a faint elongated galaxy and north of a fainter galaxy (see Supplementary Fig. 1). We have measured a redshift of $z = 0.22$ for the galaxy to the east and $z = 0.078$ for the galaxy to the south, which rules out any association of these galaxies with the supernova ($z = 0.0666$; see below).

Our spectroscopic coverage of SN2002ic encompasses a period of ~60 days, and clearly demonstrates that this object belongs to the Ia class (see Fig. 1). The features in SN2002ic are very much like those of the type Ia SN1991T⁵, but diluted in strength. Although SN1991T/1999aa-like events are sometimes referred to as 'peculiar', they make up 20% of the local population of type Ia supernovae (SNe Ia)⁶. The most remarkable spectroscopic feature in SN2002ic is the H α emission at $z = 0.0666$. This emission is spatially unresolved with a full-width at half-maximum, FWHM, of ≤ 1.2 arcsec (1.7 kpc for $H_0 = 65 \text{ km s}^{-1} \text{ Mpc}^{-1}$). The H α profiles (Fig. 2) have an unresolved (FWHM $< 300 \text{ km s}^{-1}$) component on top of a broad (FWHM $\approx 1,800 \text{ km s}^{-1}$) base. While the narrow component could be an unrelated H II region, the broader component cannot be explained in this way. Such narrow + broad H α profiles have no precedent among SNe Ia³, but are typical of SNe IIn⁷ where it is thought that the narrow lines arise from the un-shocked circumstellar material (CSM) photoionized by radiation from the SN, while the intermediate width lines are formed in the shock-heated CSM^{8,9}. The origin of the CSM in SNe IIn is attributed to the SN progenitor, a presumably massive star that undergoes mass loss before explosion. By analogy, the double component H α profile in SN2002ic is clear evidence for a dense CSM. The measured H α

fluxes in SN2002ic correspond to energies of $\sim 2 \times 10^{40} \text{ erg s}^{-1}$ in each of the broad and narrow line components. Photoionization models for the narrow component³ imply an unexpectedly high mass-loss rate of $\sim 10^{-2.4} M_{\odot} \text{ yr}^{-1}$ (where M_{\odot} is the solar mass). The absence of a rapid dimming in H α or a change in linewidth (Fig. 2) suggests that the SN/CSM interaction remains strong at least 2 months after explosion, which is also consistent with large mass-loss rates³.

The SN/CSM interaction in SNe IIn produces a luminosity enhancement compared to classical SNe II¹⁰ owing to the conversion of kinetic energy into continuum radiation. This suggests that the absorption features and light curves of SN2002ic may be similarly 'veiled' relative to 'normal' SNe Ia. This hypothesis is confirmed from the spectroscopic comparison between SN2002ic and the type Ia SN1999ee¹¹ (Fig. 3), and the photometric analysis shown in Fig. 4.

The strength of the SN/CSM interaction in SN2002ic is totally unexpected for a SN Ia, but is typical in SNe IIn. It is interesting to hypothesize that some SNe IIn may actually be SNe Ia like SN2002ic,

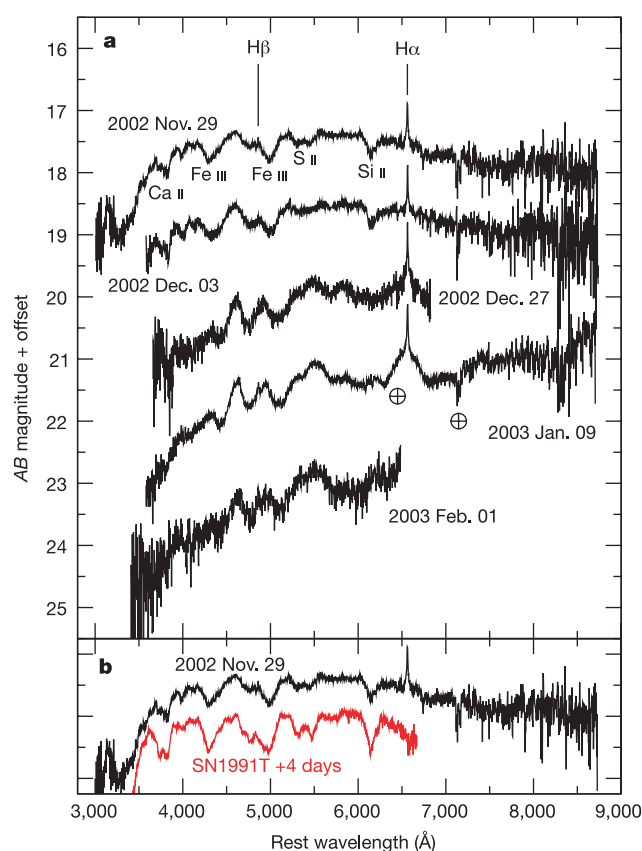


Figure 1 Spectroscopic evolution of SN2002ic. **a**, This sequence shows five spectra of SN2002ic (in AB magnitudes) obtained between 2002 November 29 and 2003 February 1 UT with the Las Campanas Observatory Baade 6.5-m and du Pont 2.5-m telescopes, and the Steward Observatory Bok 2.3-m telescope. Arbitrary offsets have been added to the spectra for clarity. The spectra are +6, +10, +34, +47 and +70 days from estimated maximum light. We attempted to remove the two most prominent telluric lines (indicated with the crossed circles), but some residuals are evident. The top spectrum shows the Si II $\lambda 6,355$ feature that defines the Ia class, as well as prominent Fe III absorption features at 4,200 and 4,900 Å. The absence of the He/Na feature at 5,900 Å in the spectral evolution rules out a type Ib/c classification. **b**, A comparison between the 2002 November 29 (+6 days) observation of SN2002ic and the spectrum of the type Ia SN1991T⁵ obtained at an epoch of +4 days, shows that both spectra are quite similar, except that the features in SN2002ic are all diluted in strength.

but with an even stronger SN/CSM interaction. In this context, we draw attention to the type IIn SN1997cy that may have been associated with the γ -ray burst source GRB970514^{12,13}. In Fig. 5 we show that the late-time (~ 70 day) spectra of SN2002ic and SN1997cy are strikingly similar. Both the *BV* light curve decline rates (~ 0.7 mag per 100 days) and the peak absolute magnitude of $M(V) \approx -20.1$ of SN1997cy¹³ are very similar to the decline rates inferred for the SN/CSM interaction and the peak brightness for SN2002ic (see Fig. 4). Note that similar high luminosities and flat, constant-colour light curves were also seen in the SN IIn 1988Z¹⁴.

The photometric properties of SN1997cy are well reproduced by a model of the explosion of a $25 M_{\odot}$ star with high explosion energy (3×10^{52} erg) which interacts with a dense CSM of $\sim 5 M_{\odot}$ (ref. 13). In this model, the light curve is powered by the SN/CSM interaction with a contribution of radioactive heating of up to $0.7 M_{\odot}$ of ^{56}Ni . In view of the close similarity between SN1997cy and SN2002ic, and the clear evidence that SN2002ic was a bona fide SN Ia, a re-examination of possible models for SN1997cy seems worthwhile, including both its association to GRB970514 and the overall energetics. We note that C/O Chandrasekhar white dwarfs are

very unlikely to produce more than 2×10^{51} erg (ref. 15). This upper limit appears to be in conflict with the total radiated energy of 10^{52} erg estimated for the SN IIn 1988Z¹⁶, but this estimate is highly uncertain.

Is there evidence for a SN/CSM interaction in other SNe Ia? It has been observed that the *BVRI* light curves of the 1991T/1999a type⁶ show an 'over-brightness' ~ 1 month after maximum compared to spectroscopically 'normal' SNe Ia^{17,18}. Perhaps all 1991T/1999aa events occur in progenitors with a significant CSM, and the SN/CSM interaction accounts for the additional luminosity at later epochs. A test of this hypothesis would be to search for radio or X-ray emission from these SNe Ia or extremely faint hydrogen emission.

The modelling of SN1997cy shows that a few solar masses of CSM material are involved in the emission processes. By analogy, we would expect a star in the progenitor system of SN2002ic to lose a similar amount of mass, ruling out a double-degenerate model for the progenitor of this type Ia explosion. A progenitor consistent with this amount of mass loss is a binary system containing a C/O white dwarf and a massive ($3\text{--}7 M_{\odot}$) asymptotic-giant-branch star

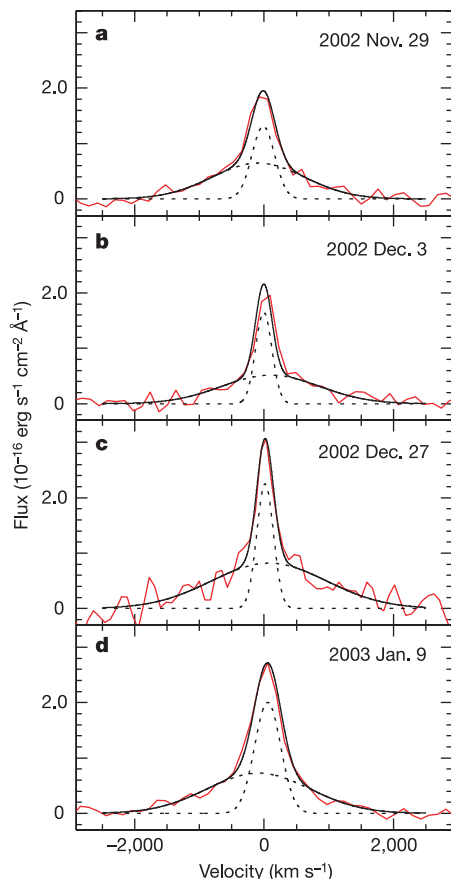


Figure 2 Decomposition and evolution of the $H\alpha$ profiles. The observed $H\alpha$ profiles are shown in red for four different epochs. These profiles cannot be fitted with single gaussian models, but two gaussians of different widths do provide acceptable fits. The black dotted lines show the individual components (with FWHM ~ 300 and $\sim 1,800 \text{ km s}^{-1}$) and the black solid lines the sum of both gaussians. This figure suggests that the $H\alpha$ profile does not evolve rapidly with time. It is difficult to make more precise statements because, while the subtraction of the continuum at early epochs is straightforward, at later times the SN has a broad emission feature (see Fig. 1a) which makes the subtraction much more uncertain.

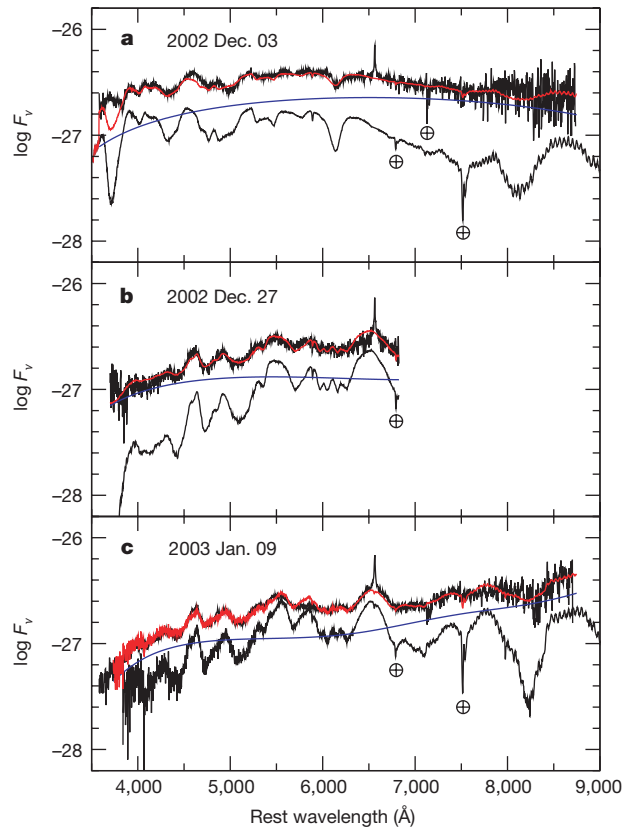


Figure 3 Spectral analysis of SN2002ic. **a**, Spectrum of SN2002ic taken on 2002 December 3 UT (heavy black line) compared with that of the normal type Ia SN 1999ee¹¹ taken 6 days past maximum (thin black line). In red is shown the sum (by eye) of a low-order continuum (blue line) and the spectrum of SN1999ee. The most prominent telluric lines are indicated with crossed circles. **b**, Same as above, except comparing the spectrum of SN2002ic obtained on 2002 December 27 UT with that of SN1999ee taken 34 days past maximum. **c**, Same as above, except comparing the spectrum of SN2002ic taken on 2003 January 9 UT with that of SN1990N obtained 47 days past maximum. Except for the features of Ca II at 3,950 Å and 8,600 Å, which appear weaker in SN2002ic, in all three cases the continuum + SN spectra and the SN2002ic spectra match extremely well. This simple model explains why the absorption features in SN2002ic appear 'veiled' relative to normal SNe Ia.

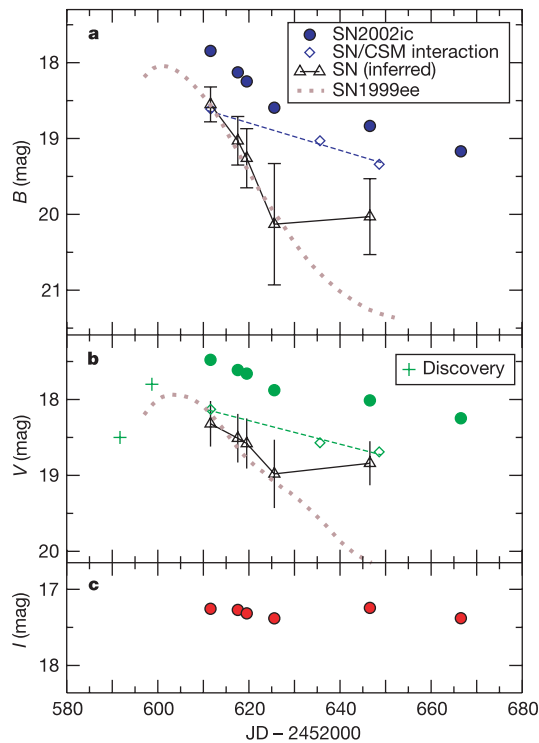


Figure 4 Photometric analysis of SN2002ic. Filled circles, light curves of SN2002ic obtained with the Las Campanas 2.5-m and 1-m telescopes (**a**, B band; **b**, V band; **c**, I band). These light curves were derived from differential measurements relative to several local standards calibrated on two photometric nights. Also shown with the 'plus' symbols in **b** are the unfiltered discovery magnitudes⁴. Maximum light occurred around November 23 (JD 2452602) and the peak magnitudes were $B \approx 17.7$, $V \approx 17.4$ and $I \approx 17.2$. Correcting for a Galactic reddening of $E(B - V) = 0.073$ (ref. 22) and K corrections²³, we derive absolute magnitudes of $M(B) \approx -20.1$, $M(V) \approx -20.3$ and $M(I) \approx -20.4$ ($H_0 = 65$), which are ~ 1 mag brighter than the most luminous SNe Ia²⁴. For comparison are plotted the B and V light curves of the 'normal' type Ia SN1999ee²⁵ (characterized by a post-maximum decline rate, $\Delta m_{15}(B)$, of 0.94) expected for the redshift and reddening of SN2002ic. While the initial decline rate of SN2002ic was very slow, the B and V light curves evolved into the final linear decline rate within ~ 25 days of maximum, which is only observed for the fastest declining SNe Ia²⁶. Also shown (diamonds) in B and V is the luminosity evolution of the SN/CSM interaction as inferred from the dilution of the spectral features (Fig. 3) to which we have fitted straight lines (shown as dashes). The triangles show the result of subtracting this light curve from the observed photometry of SN2002ic. For the first ~ 25 days, the 'unveiled' peak magnitudes of $B \approx V \approx 18.0$ are consistent with a 'normal' SN Ia. However, beyond JD 2452630 the residual flux remains high compared to SN1999ee. This suggests that a model of the light curves of SN2002ic as the sum of a 'normal' SN Ia and a slow-declining SN/CSM interaction may be overly simple.

where the integrated mass loss can reach a few solar masses¹⁹. The accretion of part of this wind onto the white dwarf could bring it to the Chandrasekhar mass. An alternative explanation is the thermonuclear explosion of the degenerate core of a 'single' asymptotic-giant-branch star in a 'type 1.5' event²⁰, although the spectrum of this event has not been calculated in detail. We also note that SN2002ic was much more luminous than its (yet-to-be-identified) host galaxy. Curiously, the host galaxy of SN1997cy was also of very low luminosity¹², as was the host of the 1999aa-like SN1999aw¹⁸. Such low-luminosity galaxies are likely to be characterized by low metallicities²¹. Hence, the presence of SN/CSM interaction in 1991T/1999aa-like events such as SN2002ic may be related to mass loss in a metal-poor environment. □

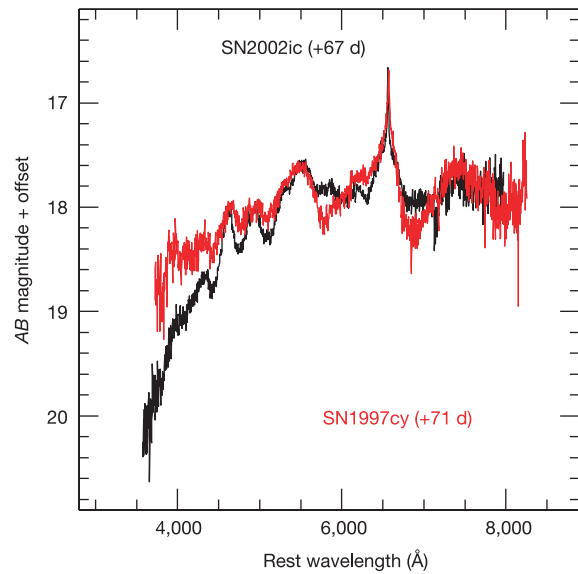


Figure 5 Spectroscopic comparison between SN2002ic and SN1997cy. Spectrum of SN2002ic taken on January 9 (~ 47 days after maximum light, which corresponds to ~ 67 days after explosion for an assumed time of 20 days between explosion and peak brightness) compared to that of the type IIa SN 1997cy taken 71 days after explosion¹³, which is assumed to coincide with the detection of GRB970514¹². The striking similarity between these two objects suggests that some SNe IIa are the result of thermonuclear explosions of white dwarfs surrounded by a dense CSM instead of core collapse in massive stars.

Received 2 April; accepted 16 June 2003; doi:10.1038/nature01854.

1. Livio, M. in *Supernovae and Gamma-Ray Bursts* (eds Livio, M., Panagia, N. & Sahu, K.) 334–335 (STScI Symp. Vol. 13, Cambridge Univ. Press, Cambridge, 2001).
2. Lentz, E. J., Baron, E., Hauschildt, P. H. & Branch, D. Detectability of hydrogen mixing in type Ia supernova premaximum spectra. *Astrophys. J.* **580**, 374–379 (2002).
3. Cumming, R. J., Lundqvist, P., Smith, L. J., Pettini, M. & King, D. Circumstellar H α from SN 1994D and future type Ia supernovae: an observational test of progenitor models. *Mon. Not. R. Astron. Soc.* **283**, 1355–1360 (1996).
4. Wood-Vasey, W. M. et al. Supernova 2002ic. *IAU Circ. No.* 8019 (2002).
5. Phillips, M. M. et al. SN 1991T: Further evidence of the heterogeneous nature of type Ia supernovae. *Astron. J.* **103**, 1632–1637 (1992).
6. Li, W. et al. A high intrinsic peculiarity rate among type Ia supernovae. *Astrophys. J.* **546**, 734–743 (2001).
7. Schlegel, E. M. A new subclass of type II supernovae? *Mon. Not. R. Astron. Soc.* **244**, 269–271 (1990).
8. Chugai, N. N. The origin of supernovae with dense winds. *Astron. Rep.* **41**, 672–681 (1997a).
9. Chugai, N. N. Supernovae in dense winds. *Astrophys. Space Sci.* **252**, 225–236 (1997b).
10. Hamuy, M. in *Core Collapse of Massive Stars* (ed. Fryer, C. L.) (Kluwer, Dordrecht, in the press); preprint at (<http://xxx.lanl.gov/astro-ph/0301006>) (2003).
11. Hamuy, M. et al. Optical and infrared spectroscopy of SN 1999ee and SN 1999ex. *Astron. J.* **124**, 417–429 (2002).
12. Germany, L. M., Reiss, D. J., Sadler, E. M., Schmidt, B. P. & Stubbs, C. W. SN 1997cy/GRB 970514: A new piece in the gamma-ray burst puzzle? *Astrophys. J.* **533**, 320–328 (2000).
13. Turatto, M. et al. The properties of supernova 1997cy associated with GRB 970514. *Astrophys. J.* **534**, L57–L61 (2000).
14. Turatto, M. et al. The type II supernova 1988Z in MCG + 03-28-022: Increasing evidence of interaction of supernova ejecta with a circumstellar ring. *Mon. Not. R. Astron. Soc.* **262**, 128–140 (1993).
15. Arnett, D. *Supernovae and Nucleosynthesis* (Princeton Univ. Press, Princeton, 1996).
16. Aretxaga, I. et al. SN 1988Z: Spectro-photometric catalogue and energy estimates. *Mon. Not. R. Astron. Soc.* **309**, 343–354 (1999).
17. Suntzeff, N. B. in *Supernovae and Supernova Remnants* (eds McCray, R. & Wang, Z.) 41 (IAU Colloq. 145, Cambridge Univ. Press, Cambridge, 1996).
18. Strolger, L.-G. et al. The type Ia supernova 1999aw: A probable SN 1999aa-like event in a low luminosity host galaxy. *Astron. J.* **124**, 2905–2919 (2002).
19. Weidemann, V. Revision of the initial-to-final mass relation. *Astron. Astrophys.* **363**, 647–656 (2000).
20. Iben, I. & Renzini, A. Asymptotic giant branch evolution and beyond. *Annu. Rev. Astron. Astrophys.* **21**, 271–342 (1983).
21. Henry, R. B. C. & Worthey, G. The distribution of heavy elements in spiral and elliptical galaxies. *Publ. Astron. Soc. Pacif.* **111**, 919–945 (1999).
22. Schlegel, D. J., Finkbeiner, D. P. & Davis, M. Maps of dust infrared emission for use in estimation of reddening and cosmic microwave background radiation foregrounds. *Astrophys. J.* **500**, 525–553 (1998).
23. Hamuy, M., Phillips, M. M., Wells, L. A. & Maza, J. K. corrections for type Ia supernovae. *Publ. Astron. Soc. Pacif.* **105**, 787–793 (1993).

24. Phillips, M. M. *et al.* The reddening-free decline rate versus luminosity relationship for type Ia supernovae. *Astron. J.* **118**, 1766–1776 (1999).
25. Stritzinger, M. *et al.* Optical photometry of the type Ia SN 1999ee and the type Ib/c SN 1999ex in IC 5179. *Astron. J.* **124**, 2100–2117 (2002).
26. Hamuy, M. *et al.* The morphology of type Ia supernovae light curves. *Astron. J.* **112**, 2438–2447 (1996).

Supplementary Information accompanies the paper on www.nature.com/nature.

Acknowledgements All the co-authors participated in gathering the observations of the supernova. M.H. noticed the presence of hydrogen emission. M.M.P. noticed spectroscopic and photometric peculiarities and put forward the idea that these could be understood as due to SN/CSM interaction. N.B.S. provided the arguments about the progenitor types. M.H., M.M.P. and N.B.S. co-wrote this Letter. M.H. is a Hubble Fellow.

Competing interests statement The authors declare that they have no competing financial interests.

Correspondence and requests for materials should be addressed to M.H. (mhamuy@ociw.edu).

Ballistic carbon nanotube field-effect transistors

Ali Javey¹, Jing Guo², Qian Wang¹, Mark Lundstrom² & Hongjie Dai¹

¹Department of Chemistry, Stanford University, California 94305, USA

²School of Electrical and Computer Engineering, Purdue University, West Lafayette, Indiana 47907, USA

A common feature of the single-walled carbon-nanotube field-effect transistors fabricated to date has been the presence of a Schottky barrier at the nanotube–metal junctions^{1–3}. These energy barriers severely limit transistor conductance in the ‘ON’ state, and reduce the current delivery capability—a key determinant of device performance. Here we show that contacting semiconducting single-walled nanotubes by palladium, a noble metal with high work function and good wetting interactions with nanotubes, greatly reduces or eliminates the barriers for transport through the valence band of nanotubes. *In situ* modification of the electrode work function by hydrogen is carried out to shed light on the nature of the contacts. With Pd contacts, the ‘ON’ states of semiconducting nanotubes can behave like ohmically contacted ballistic metallic tubes, exhibiting room-temperature conductance near the ballistic transport limit of $4e^2/h$ (refs 4–6), high current-carrying capability ($\sim 25 \mu\text{A}$ per tube), and Fabry–Perot interferences⁵ at low temperatures. Under high voltage operation, the current saturation appears to be set by backscattering of the charge carriers by optical phonons. High-performance ballistic nanotube field-effect transistors with zero or slightly negative Schottky barriers are thus realized.

Transparent electrical contacts made to metallic single-walled carbon nanotubes (SWNTs) have revealed them to be ballistic conductors that exhibit two units of quantum conductance $4e^2/h$ ($R_Q = h/4e^2 = 6.5 \text{ k}\Omega$)^{4–6}. Carrier transport through the valence and conduction bands of a high-quality semiconducting SWNT could also be ballistic, presenting an opportunity to realize ballistic field-effect transistors (FETs) based on molecular electronic materials. However, such effort has been hampered by non-ideal electrical contacts made to semiconducting SWNTs. Previously, thermionic emission current and associated barriers between Ni contacts and SWNTs⁷ have been reported for materials grown by chemical vapour deposition (CVD). Recently, significant Schottky barriers (SBs) have been found in SWNT-FETs (with Ti contacts and laser-oven nanotubes)^{1–3}. Thermionic emission and tunnelling are involved in transport across the SBs, which limits the ON state

conductance of nanotube FETs to be well below the $4e^2/h$ limit ($G_{\text{ON}} \approx 0.001 \times 4e^2/h$ for laser tubes^{1–3}; and $G_{\text{ON}} \approx (0.05 - 0.3) \times 4e^2/h$ for CVD tubes^{7–10}) at room temperature. At low temperatures, quenching of thermionic currents causes semiconducting SWNT devices to be about 10–100 times more resistive than at room temperature^{7,11,12}.

A solution is presented here to eliminate or greatly suppress SBs at metal–nanotube contacts. We find that for Pd-contacted, long, semiconducting SWNT devices (length $L = 3 \mu\text{m}$, diameter $d \approx 3 \text{ nm}$, Fig. 1a) with back gates (SiO_2 thickness $t_{\text{ox}} = 500 \text{ nm}$), the room-temperature ON state conductance through the valence band (VB) is up to $G_{\text{ON}} \approx 0.1 \times (4e^2/h)$ ($R_{\text{ON}} = 60 \text{ k}\Omega$, Fig. 1b). For short channel nanotubes at room temperature ($L = 300 \text{ nm}$, Fig. 1a), $G_{\text{ON}} = (0.4 - 0.5) \times (4e^2/h)$ ($R_{\text{ON}} = 13 \text{ k}\Omega$, Fig. 1c). For long SWNTs, the ON state p-channel conductance exhibits metallic behaviour between room temperature and $\sim 200 \text{ K}$, and typically shows a downturn in G_{ON} upon further cooling (Fig. 1b inset). The short nanotubes do not show such downturn, and the average G_{ON} monotonically increases as temperature T decreases to $\sim 50 \text{ K}$ (Fig. 1d), below which pronounced oscillations with Fabry–Perot type of interferences⁵ appear in the G versus gate voltage (V_{gs}) data

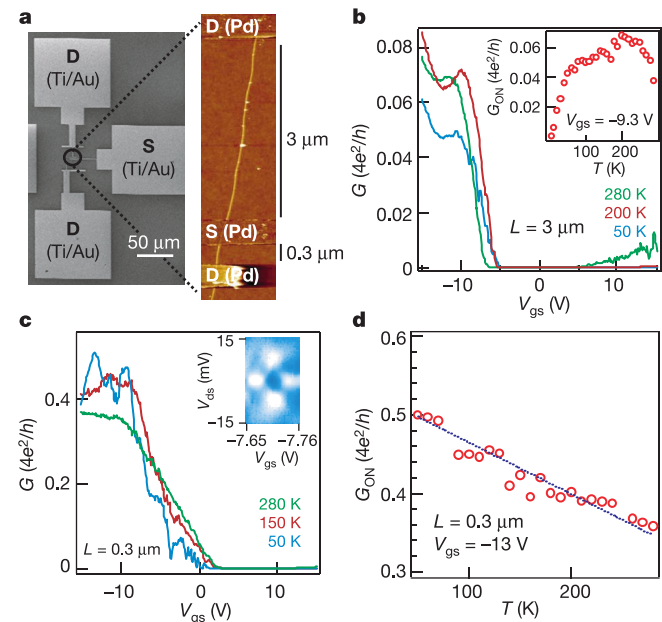


Figure 1 Pd-contacted long ($L = 3 \mu\text{m}$) and short ($L = 300 \text{ nm}$) back-gated SWNT devices formed on the same nanotubes on SiO_2/Si . **a**, A scanning electron microscope (SEM) image (left) and atomic force microscope (AFM) image (right) of a representative device. CVD synthesis for SWNTs and device fabrication were as described previously^{25,26}, except that Pd was used to contact nanotubes. The catalyst used here gave a wide range of nanotube diameters ($1.2 - 5 \text{ nm}$)²⁵. Ti/Au metal bonding pads were used to connect to the Pd source (S) and drain (D) electrodes. (We note that Pd electrodes tended to be soft and not robust against electrical probing). The devices were annealed in Ar at 225°C for 10 min after fabrication. The thickness of SiO_2 gate dielectric was $t_{\text{ox}} = 500 \text{ nm}$, except for the devices in Fig. 4 with $t_{\text{ox}} = 67 \text{ nm}$. AFM topographic height measurements were used to determine the diameters of SWNTs. The electrical data shown here were recorded with the devices placed in vacuum. **b**, G (at low S–D bias V_{ds}) versus gate voltage V_{gs} for a $3 \mu\text{m}$ -long SWNT ($d \approx 3.3 \text{ nm}$) device recorded at various T . Inset, G_{ON} versus T for the device. **c**, G versus V_{gs} for a 300 nm -long tube section on the same tube as for **b** at various T . Differential conductance $dI_{\text{ds}}/dV_{\text{ds}}$ versus V_{ds} and V_{gs} (inset, measured by a lock-in technique) at $T = 1.5 \text{ K}$ shows a Fabry–Perot-like interference pattern (bright peak $G \approx 4e^2/h$, dark region $G = 0.5 \times 4e^2/h$). Note that in certain V_{gs} regions, the pattern appears irregular, a phenomenon also seen for Fabry–Perot interference in metallic tubes⁵. **d**, G_{ON} versus T for the $L = 300 \text{ nm}$ semiconducting tube down to $\sim 50 \text{ K}$.